Proceedings of the 2nd Croatian Conference on Earthquake Engineering - 2CroCEE
Zagreb, Croatia - March 22 to 24, 2023
Copyright © 2023 CroCEE
DOI: https://doi.org/10.5592/CO/2CroCEE.2023.26

EXPERIENCES IN MODELING AND ANALYSIS OF MINE SEAL STRUCTURES

Viktor Hristovski [(1)], Emil Jankulovski [(2)], John Burke[(3)]

[(1)] *Professor, Ss. Cyril and Methodius University in Skopje, Institute of Earthquake Engineering and Engineering Seismology UKIM-IZIIS Skopje, P.O. Box 101, 165 Todor Aleksandrov Str., 1000 Skopje, Republic of Macedonia, viktor@iziis.ukim.edu.mk*

[(2)] *BE, ME, MIE Aust, Director, INDUCTA Pty Ltd, PO Box A2293, Sydney South, NSW Australia 1235, emil@inducta.com.au*

[(3)] *BE CPEng NER Civil/Structural, MIE Australia, Director, Burke Engineering Services P/L, Thornton, Australia*

Abstract

Mine seals are structures used to serve as protection shields against short term instantaneous pressure loadings like blasts, which could occur in underground mine workings during serviceability period in combination with possible hydrostatic pressure from ground water. They can also resist accidental loads, like earthquakes, that may occur during the excavation period. In this paper, experiences in modelling and nonlinear finite element analysis of mine seal structures that have preceded the design phase are presented. Namely, for the period of 10 years, more than 20 study cases of mine seals have been modelled and analysed by the authors. Each separate study case consisted of a number of different model types, depending on various assumptions about prescribed boundary conditions, material used, seal structure adopted, prescribed loading, existence of bolts, existence of openings, etc. For all cases, there have been performed force-displacement progressive failure analyses (PFM), with detailed description of the failure mechanism and critical points on the obtained diagrams. The design force-displacement diagrams have been constructed by using an overstrength factor and a material partial safety coefficient. The design limit states criteria have been defined for each study case taken separately. All study cases are presented comparatively in a tabular form according to the material and geometrical properties, failure mechanisms and design limit state criteria. The numerical analyses have been performed by using the software package FELISA/3M. Willam-Warnke and Drucker-Prager elastic-plastic criteria have been used to account for the material nonlinearity. Models have been built using SOLID iso-parametric finite elements with 20 nodes for modelling of the seal body and LINK elements for modelling of the contact surfaces between the body and the surrounding rocks. This study is believed to have given a valuable insight into modelling and methods for analysis of mine seals structures, useful for practitioners in this field.

Keywords: Mine seals, finite element method, nonlinear analysis, failure analysis, backward Euler scheme

1. Introduction

The purpose of mine seal structures is to isolate abandoned mine tunnels from still active mining workings (see Fig. 1). Namely, mine seals should prevent spreading of possible explosions from the abandoned areas into the active workings. Also, they may be designed to prevent the leakage of potentially explosive or toxic gases, or their migration into the active zones. The bearing system of the seal structures and the material from which it is made can be quite different, depending on the in-situ conditions. The technology of construction and the very design of the seal structures is a special topic of research [1,2] that should follow appropriate technical norms, depending on the country in which they are constructed. In this work, we will not deal with the technology and design phases themselves, rather than with the numerical modelling and analysis of the mine seal structures using the finite element method (FEM). It should be noted that, presently, this topic is very much of interest. Namely, it is anticipated that a huge number of underground mines in the world will be closed in near future because of the global climate change problem. This will require these types of seals.

With the recent technical norms in the world the level of seal design requirements and criteria related to the strength of the constructed mine seals have been increased [1, 2]. These requirements can be best

Proceedings of the 2nd Croatian Conference on Earthquake Engineering - 2CroCEE
Zagreb, Croatia - March 22 to 24, 2023
Copyright © 2023 CroCEE
DOI: https://doi.org/10.5592/CO/2CroCEE.2023.26

satisfied if the seal design includes the following three phases: laboratory testing, in-situ testing, and FEM nonlinear analysis. Usually, the properties of the proposed construction material are determined by laboratory tests. In addition, the in-situ testing provides the remaining input parameters for numerical finite element modelling related to properties of the surrounding rock deposit, conditions at the contact zones between the rock deposit and the seal structure, possible hydrostatic pressure level, the level of the risk pertaining to explosions, etc. Finally, FEM nonlinear analysis can simulate the failure mechanism of the seal structure based on the input parameters from the tests. According to the National Institute for Occupational Safety and Health (NIOSH) [1], the following failure modes of the mine seal structures are possible and permitted: (1) bending and tensile failure through the seal structure, (2) shear failure through the seal foundation, (3) shear failure along the seal-foundation interface, and (4) shear failure through the seal. Finite element numerical modelling and nonlinear parametric analysis can serve for control of the resulting failure modes and proportioning the mine seal structures (usually the seal thickness is the unknown parameter). To achieve these goals, push-over progressive failure analysis (PFA) for obtaining the force-displacement curve has been the basic task in the research.

Figure 1. a) Drift seal built of concrete, b) Tunnel seal with doors

The paper is organised as follows: In the subsequent Chapter 2, the adopted numerical finite element models, the material elastic-plastic constitutive relationships and the implemented computational stress-update methods are discussed. Discussion about the design criteria adopted in the analyses, depending on the obtained progressive failure mechanisms (PFM) is given in Chapter 3. In Chapter 4, a detailed comparative review of the performed analyses is made, describing and classifying them according to prescribed boundary conditions, adopted seal bearing structure, material used, prescribed loading, existence of bolts, existence of openings, obtained failure mechanism, etc. Then, conclusions and a table of consulted references are given.

2. Numerical modelling of mine seal structures

2.1 Finite element discretization

To accomplish the required goals – determination of the failure mode type and the seal thickness, a proper nonlinear finite element incremental force-displacement (or push-over) analysis is necessary. Nonlinear finite element modelling and analysis is generally a complex and a responsible task, especially for structures like mine seals built of concrete-like or foam-like materials. In this chapter, the assumptions regarding the developed finite element models and the used material models for the analysed structures are discussed in more details.

To get an insight into the total spatial distribution of the stresses and deformations in the seal structure, three-dimensional models that include 3D solid iso-parametric mapped elements for the seal body have been used for all study cases. The used solid elements have 20 nodal points and 3x3x3=27 Gaussian points that have been used for numerical integration. Each nodal point has 3 translational degrees of freedom (DOFs). In the cases where the contact zones are modelled, 3D link elements with two nodal

Proceedings of the 2nd Croatian Conference on Earthquake Engineering - 2CroCEE
Zagreb, Croatia - March 22 to 24, 2023
Copyright © 2023 CroCEE
DOI: https://doi.org/10.5592/CO/2CroCEE.2023.26

points are used, each with 3 translation DOFs. If models contain steel bolts, then 3D truss elements are also used to model them. The finite element mesh for all cases has been generated by using a special pre-processor software for automatic generation of the prescribed 3D domain with solid iso-parametric elements, considering the openings, and also including the link and truss elements, if necessary.

2.2 Elastic-plastic material modelling

Having in mind the properties of the materials, plasticity-based material models have been adopted. For seals built of concrete-like materials (as plaster only, plaster plus cement, "flexus" material, etc.) the three-parameter Willam-Warnke model of concrete formulation [3-8] has been adopted. Also, for seals built of Silcrete Thin Skin Lining (TSL) two-component material, the Willam-Warnke three-parameter yield criterion has proved to be convenient. On the other hand, the so called Rocksil (foam-like) material has been modelled by using the Drucker-Prager yield criterion [5-8]. In the following, we will focus on the numerical solution for the mentioned two elastic-plastic models, especially on the use of the so-called backward-Euler return method for stress update integration.

If the yield surface f is presented as a function of invariants I_1, i.e., the first stress tensor invariant, J_2 and J_3, i.e., the second and the third stress deviator tensor invariants, then the flow vector $\boldsymbol{a}$ can be determined using the following relation [10]:

$$\boldsymbol{a} = \frac{\partial f}{\partial \boldsymbol{\sigma}} = C_1\boldsymbol{a}_1 + C_2\boldsymbol{a}_2 + C_3\boldsymbol{a}_3 = C_1\frac{\partial I_1}{\partial \boldsymbol{\sigma}} + C_2\frac{\partial J_2}{\partial \boldsymbol{\sigma}} + C_3\frac{\partial J_3}{\partial \boldsymbol{\sigma}} \tag{1}$$

where the coefficients C_i depend on the yield function f adopted. For known tensor of stresses in Cartesian coordinates adopted in the vector form:

$$\boldsymbol{\sigma}^T = \{\sigma_x \quad \sigma_y \quad \sigma_z \quad \tau_{xy} \quad \tau_{yz} \quad \tau_{zx}\} \tag{2}$$

the partial derivatives in Eq. (1) depend only on the stress state, and they can be easily derived. Eq. (1) is sufficient to enable the forward-Euler method for stress update integration to be applied to the different yield criteria. However, to implement the backward Euler return method, differentiating of the flow vector $\boldsymbol{a}$ with respect to stresses $\boldsymbol{\sigma}$ is necessary, in which case we obtain:

$$\frac{\partial \boldsymbol{a}}{\partial \boldsymbol{\sigma}} = C_2\frac{\partial \boldsymbol{a}_2}{\partial \boldsymbol{\sigma}} + C_3\frac{\partial \boldsymbol{a}_3}{\partial \boldsymbol{\sigma}} + C_{22}\boldsymbol{a}_2\boldsymbol{a}_2^T + C_{23}\boldsymbol{a}_2\boldsymbol{a}_3^T + C_{32}\boldsymbol{a}_3\boldsymbol{a}_2^T + C_{33}\boldsymbol{a}_3\boldsymbol{a}_3^T \tag{3}$$

where $\frac{\partial \boldsymbol{a}_2}{\partial \boldsymbol{\sigma}}$ and $\frac{\partial \boldsymbol{a}_3}{\partial \boldsymbol{\sigma}}$ can be easily found. For Drucker-Prager yield criterion, given in the following form:

$$f = DI_1 + J_2^{1/2} - \sigma_0 \tag{4}$$

where D and σ_0 are constants, the coefficients in Eqs. (1) and (3) will be as follows [9,10]:

$$C_1 = D, \quad C_2 = \frac{1}{2}J_2^{-1/2}, \; C_3 = 0, \; C_{22} = -\frac{1}{4}J_2^{-3/2}, \; C_{23} = C_{32} = C_{33} = 0 \tag{5}$$

The obtaining of the coefficients C_i and C_{ij} for the yielding surface of Willam-Warnke three-parameter elastic-perfect plastic model is much more complicated. It has been conducted by the first author and the resulting coefficients have been implemented in the FELISA/3M computer software [11]. The yield surface of Willam-Warnke three parametric criterion has straight meridians and is expressed by means of average stresses σ_m, τ_m and the angle of similarity θ has the following form [3,5]:

$$f(\sigma_m, \tau_m, \theta) = \frac{1}{\rho}\frac{\sigma_m}{f_c'} + \frac{1}{r(\theta)}\frac{\tau_m}{f_c'} - 1 = 0 \tag{6}$$

where:

$$\sigma_m = \frac{I_1}{3}, \tau_m = \sqrt{\frac{2}{5}J_2} \tag{7}$$

Proceedings of the 2nd Croatian Conference on Earthquake Engineering - 2CroCEE
Zagreb, Croatia - March 22 to 24, 2023
Copyright © 2023 CroCEE
DOI: https://doi.org/10.5592/CO/2CroCEE.2023.26

and f_c' is uniaxial compressive strength of the material (concrete). In the yield surface (6), $r(\theta)$ is the radius of the elliptic trace of the failure surface for $0 \leq \theta \leq 60^0$, with angle of similarity θ defined in terms of invariants by the following expression [5,7]:

$$\cos 3\theta = \frac{3\sqrt{3}}{2}\frac{J_3}{J_2^{-3/2}} \tag{8}$$

The solution of the coefficients C_i and C_{ij} has been conducted in terms of three parameters ρ, r_t and r_c. The three parameters ρ, r_t and r_c can be identified by the three typical concrete tests: the uniaxial-tension test, the uniaxial compression test and the equal-biaxial-compression test. Using the normalized strength values:

$$\bar{f}_t' = \frac{f_t'}{f_c'} \text{ and } \bar{f}_{bc}' = \frac{f_{bc}'}{f_c'} \tag{9}$$

where f_t' is the uniaxial tension concrete strength, and f_{bc}' is equival-biaxial-compression concrete strength, the three parameters can be found by the following relations [3,5]:

$$\rho = \frac{\bar{f}_{bc}'\bar{f}_t'}{\bar{f}_{bc}'-\bar{f}_t'} \tag{10}$$

$$r_t = \left(\frac{6}{5}\right)^{1/2}\frac{\bar{f}_{bc}'\bar{f}_t'}{2\bar{f}_{bc}'+\bar{f}_t'} \tag{11}$$

$$r_c = \left(\frac{6}{5}\right)^{1/2}\frac{\bar{f}_{bc}'\bar{f}_t'}{3\bar{f}_{bc}'\bar{f}_t'+\bar{f}_{bc}'-\bar{f}_t'} \tag{12}$$

The differentiation of the yield function (6) with respect to stresses $\boldsymbol{\sigma}$, having in mind the relation (8) for similarity angle θ, leads to the final coefficients C_i, as follows:

$$C_1 = \frac{1}{3\rho f_c'} \tag{13}$$

$$C_2 = \frac{\sqrt{2}}{2\sqrt{5}}J_2^{1/2}\frac{1}{r(\theta)f_c'}\left[1-\frac{\cos 3\theta}{\sin 3\theta}\frac{dr}{d\theta}\frac{1}{r(\theta)}\right] \tag{14}$$

$$C_3 = \frac{\sqrt{6}}{\sqrt{5}}\frac{dr}{d\theta}\frac{1}{2\sin 3\theta r^2(\theta)f_c'J_2} \tag{15}$$

The differentiation of the flow vector (3) results in the following coefficients C_{ij} :

$$C_{22} = -\frac{1}{2}\lambda_1 J_2^{-3/2}A_1(\theta) - \frac{3}{2}\lambda_1 J_3 J_2^{-3}\frac{dA_1(\theta)}{d\theta}A_3(\theta) \tag{16}$$

$$C_{23} = -\frac{3}{2}\lambda_2\frac{dA_2}{d\theta}A_3(\theta)J_3J_2^{-7/2} - \lambda_2 A_2(\theta)J_2^{-2} \tag{17}$$

$$C_{32} = \lambda_1\frac{dA_1(\theta)}{d\theta}A_3(\theta)J_2^{-2} \tag{18}$$

$$C_{33} = \lambda_2\frac{dA_2}{d\theta}A_3(\theta)J_2^{-5/2} \tag{19}$$

where coefficients λ_1 and λ_2 are the following:

$$\lambda_1 = \frac{\sqrt{2}}{2\sqrt{5}}\frac{1}{f_c'} \tag{20}$$

$$\lambda_2 = \frac{\sqrt{6}}{\sqrt{5}}\frac{1}{2f_c'} \tag{21}$$

Proceedings of the 2nd Croatian Conference on Earthquake Engineering - 2CroCEE
Zagreb, Croatia - March 22 to 24, 2023
Copyright © 2023 CroCEE
DOI: https://doi.org/10.5592/CO/2CroCEE.2023.26

The functions $A_i(\theta)$ and their derivatives $\frac{dA_i(\theta)}{d\theta}$, i=1,2,3, are the following:

$$A_1(\theta) = \frac{1}{r(\theta)}\left[1 - \frac{\cos 3\theta}{\sin 3\theta}\frac{dr}{d\theta}\frac{1}{r(\theta)}\right] \tag{22}$$

$$A_2(\theta) = \frac{dr}{d\theta}\frac{1}{r^2(\theta)\sin 3\theta} \tag{23}$$

$$A_3(\theta) = \frac{\sqrt{3}}{2\sin 3\theta} \tag{24}$$

$$\frac{dA_1(\theta)}{d\theta} = -\frac{1}{r^2(\theta)}\frac{dr}{d\theta}\left[\left(1 - \frac{\cos 3\theta}{\sin 3\theta}\frac{dr}{d\theta}\frac{1}{r(\theta)}\right) - \frac{3}{\sin^2 3\theta} + \frac{\cos 3\theta}{\sin 3\theta}\frac{\frac{d^2r}{d\theta^2}}{\frac{dr}{d\theta}} - \frac{1}{r(\theta)}\frac{dr}{d\theta}\frac{\cos 3\theta}{\sin 3\theta}\right] \tag{25}$$

$$\frac{dA_2(\theta)}{d\theta} = \frac{d^2r}{d\theta^2}\frac{1}{r^2(\theta)\sin 3\theta} - \left(\frac{dr}{d\theta}\right)^2\frac{2}{r^3(\theta)\sin 3\theta} - \frac{dr}{d\theta}\frac{3\cos 3\theta}{r^2(\theta)\sin^2 3\theta} \tag{26}$$

Note that the radius vector $r(\theta)$ function can be found in [5]. Also, the expressions for partial derivatives $\frac{\partial I_1}{\partial \boldsymbol{\sigma}}$, $\frac{\partial J_2}{\partial \boldsymbol{\sigma}}$ and $\frac{\partial J_3}{\partial \boldsymbol{\sigma}}$ in Eq. (1) and Eq. (3) can be found in [10].

Together with the stress-update algorithm based on the backward-Euler return method, a procedure for calculation of the so-called consistent tangent modular matrix D_p, necessary for integration of the tangent stiffness matrix of the structure, has been developed. These two parallel computational phases have been implemented in the software package FELISA/3M [11], by which the analyses of mine seal structures were performed. It is important to note that the implementation of the backward-Euler return method resulted in much faster convergence and consistency of the results, compared to our previous experience with the forward-Euler return method.

3. Design criteria based on progressive failure analyses

The performed nonlinear finite element incremental push-over analyses have provided the force-displacement curves and the failure mechanisms for all the analysed cases. The failure modes have been used further for definition of the design criteria for determination of the seal thickness. In the construction of the force-displacement curves, the corresponding force at each incremental step has been defined as the sum of the distributed forces over the loaded surface, and the corresponding displacement has been defined as a displacement at some representative point (usually, it is the midpoint of the loaded surface). The incremental analyses have been performed using the force-controlled approach.

The main question during the analyses was how to define the "ultimate" point, or the point with maximum values of both force and displacement. Note that the practical needs directed us to construct only the ascending part of the force-displacement curve, rather than its descending part, which was the reason why the force-controlled approach was adopted in the analyses. Consequently, the final converged incremental step was supposed to be the "ultimate" point. However, the analyses were often completed prematurely due to the displacement divergence over the iteration process, before reaching the final incremental step, which was regarded as an indication of failure, although, the computations were most frequently finished normally with the convergence of the last prescribed incremental step. In the case of convergence of all incremental steps, the measure for the ultimate point was judged based on the level of the obtained progressive damage during the incremental analysis.

From the comparative review of the performed analyses given in the subsequent Chapter 4, we will see that mainly two structural systems have been adopted for the mine seals: (1) A rectangular plate resting on its four edges, loaded in-plane and out-of-plane, or (2) A complex 3D continuum structure with an adhesion-type contact between the body and the surrounding rock. The failure mechanism of the first

Proceedings of the 2nd Croatian Conference on Earthquake Engineering - 2CroCEE
Zagreb, Croatia - March 22 to 24, 2023
Copyright © 2023 CroCEE
DOI: https://doi.org/10.5592/CO/2CroCEE.2023.26

structural type has been identified usually as bending cracking (BC), while the failure mechanism of the second structural type has been identified as a shear-slip failure (SSF) at the contact. However, sometimes, as a result of variation of the geometry, a mixed failure mode (MFM) has been obtained, where principal compression stresses or principal shear stresses in the body have received maximum values. For all analyses, the progressive failure mechanism in terms of critical damage phases (points) and consequently, the adopted design criterion will be described in the chapter that follows.

4. Comparative review of performed analyses and discussion of results

4.1 Adopted materials and their properties

Analyses were performed using the FELISA/3M software package for finite element nonlinear analysis of structures [11]. The properties of the seal materials adopted in the analyses are presented in Table 1, where f_c is uniaxial compressive cylinder strength in MPa, f_t' is uniaxial tension strength in MPa, E is initial Young's modulus of elasticity in MPa, ν is Poisson's ratio, and ρ is density in [kN s^2/m^3]. The study case numbers are indicated in the second column of the table, while in the last column the yield criterion used in the elastic-plastic analysis is given, where "W-W 3" means Willam-Warnke yield surface with 3 parameters, and "D-P" means Drucker-Prager yield surface. For the case of Drucker-Prager criterion, cohesion c in [MPa] and internal friction angle φ in degrees are given in the table, instead of uniaxial tensile strength f_t'. The material properties were adopted according to the obtained results from the appropriate laboratory tests. Note that for the first two analyses of the study case number 14, where HYG 2 PACK material was used, the unknown parameter was the uniaxial compressive strength, rather than the seal thickness, so that the resulting strength from the analysis is presented in the table. The original HYG 2 PACK used for the third analysis had a compressive strength of 3,3 MPa (see HYG 2 PACK (2) in the table), in which case the seal thickness was the unknown parameter. As an illustration, a photo of Rocsil foam material (see study case 15-16) is shown in Fig. 2.

Table 1– Properties of seal materials (body) used in the analyses

Material	Study case no.	f_c	f_t'	E	ν	ρ	Yield surface
Plaster only	1	4,375	1,93	21000	0,2	2,4	W-W 3
Plaster/cement	1	9,625	2,5	21000	0,2	2,4	W-W 3
Flexus	2	50,0	5,0	17000	0,2	2,1	W-W 3
Shotcrete	2	55,0	3,8	17000	0,2	2,1	W-W 3
Concrete grout (1)	3-8	7,28	1,6	17000	0,2	2,1	W-W 3
Concrete grout (2)	9	7,28	1,09	17000	0,2	2,1	W-W 3
Concrete grout (3)	10	15,0	2,25	17000	0,2	2,1	W-W 3
Silcrete TSL (1)	11-12	35,0	10,0	750	0,49	1,1	W-W 3
Rocksil (1)	13, 17-18	50,0	c=0,0217, φ=30,2°	4,166	0,1	0,045	D-P
HYG 2 PACK (1)	14	(unknown) obtained 8,5 and 4,2	0,78	20000	0,2	1,1	W-W 3
HYG 2 PACK (2)	14	3,3	0,78	20000	0,2	1,1	W-W 3
Rocsil foam (2)	15-16	70,0	c=0,0217, φ=30,2°	5,625	0,19	0,063	D-P
Concrete grout (3)	19-20	80,0	3,72	39348	0,2	2,4	W-W 3
Silcrete TSL (2)	21	35,0	10,0	512,62	0,49	1,33	W-W 3

4.2 Failure mechanisms and design criteria

Classification related to the obtained failure mechanisms and the design criteria for some study cases is presented in Table 2. Note that for design purposes, force-displacement curves with a strength reduction factor of φ=0.75 and loading safety factor of FS=1.5 have been generally used for mostly of the

Proceedings of the 2nd Croatian Conference on Earthquake Engineering - 2CroCEE
Zagreb, Croatia - March 22 to 24, 2023
Copyright © 2023 CroCEE
DOI: https://doi.org/10.5592/CO/2CroCEE.2023.26

analyses. For some study case these values are different. In the table, bending cracking is denoted by "BC". The progressive failure mechanism is denoted by the order of occurrence of the critical damage phases (or points in the force-displacement curve). The critical point abbreviations and other abbreviations are explained in the Legend, placed on the bottom of the table. For example, for the study case no. 1, the progressive failure mechanism denoted by "TC-BC-SC-MC-CL" means that the first top cracks occurred, then the bottom cracks, the side cracks, etc. The design criterion in the table is explained by use of the value of the design pressure. For example, for the study case no. 1, the design criterion was $1.8(P_{CL}-P_{TC})$ where P_{CL} is the corresponding pressure for the collapse (ultimate) point, and P_{TC} is the corresponding pressure for the first top cracks.

Figure 2. Tunnel seal – Rocsil foam

To illustrate the modelling, analysis, and obtained progressive fracture mechanisms, we will present some results from selected study cases. In Fig. 3 the obtained progressive failure mechanism for study case no. 4 of a plate mine seal structure with an opening is presented. It can be observed that the first cracks occur on the bottom corners of the opening, then on the top of the plate and finally on the sides of the plate.

In Fig. 4 the same results are presented for study case no. 5 of a plate mine seal structure without openings. For this study case the top and bottom cracks appear first, then the side ones, and finally the middle cracks develop at the end of the failure mechanism.

Study case 5 of mine seal structure with bolts is presented in Fig. 5. Note that bolts are modelled by truss elements (denoted in green colour). The local deformations near bolts are evident in this case. The presented study cases in Figs. 1-3 have been modelled by elastic-plastic Willam-Warnke yield surface with three parameters.

In Fig. 6 the results for study case 16 is presented. Note that for this case loading safety coefficient has been adopted with value of 1.1. This study case represents a dam-like mine seal structure built of Rocksil foam material, modelled by elastic-plastic Drucker-Prager yield surface. The principal aim of the analysis was to simulate all characteristic phases of the progressive failure mechanism of the analysed system. To this end, the numerical model has been developed in such a way to grasp two failure modes: (1) sliding in the contact between the Rocksil material and the surrounding rocks; and (2) shearing in the body of the Rocksil seal material. The sliding failure mechanism in the contact has been controlled by the Mohr-Coloumb law using the friction coefficient and the bond strength as parameters, via 3D Nonlinear Link elements. The criterion for control of shear stresses in the body was based on the maximum shear stress. occurring at the analysed points. As presented in the Fig. 6, both damage mechanisms - shear failure in the body and shear-slip in the contact, developed simultaneously, however, finally, the structure collapsed in shear-slip failure mode in the contact between the seal body and the surrounding rock. In the figure, red dots denote points where principal shear stresses exceed allowable values.

Proceedings of the 2nd Croatian Conference on Earthquake Engineering - 2CroCEE
Zagreb, Croatia - March 22 to 24, 2023
Copyright © 2023 CroCEE
DOI: https://doi.org/10.5592/CO/2CroCEE.2023.26

Table 2– Failure mechanisms and design criteria for some study cases

Study case no.	Loading	Failure mechanism	Design criterion
1	SW + normal pressure 5-20 PSI	BC: TC-BC-SC-MC-CL	$1.8(P_{CL}-P_{TC})$
2	SW + normal pressure 2 PSI	BC: TC-BC-SC-MC-CL	P_{CL}
3	SW + normal pressure 4,40,100 PSI	BC: TC-BC-SC-MC-CL	P_{CL}
4	SW + normal pressure 2 PSI (plate with an opening)	BC: TC-BC-SC- CL	P_{CL}
5	SW + normal pressure 2-50 PSI (with and without bolts)	BC: TC-BC-SC-MC-CL	P_{CL}
6	SW + HP (with bolts) (with bolts in two rows, with steel door and seal crem)	/	/
7	/	/	/
8	SW + HP (two blocks with cold joints, bolts in two rows, SF=3.0, φ=0.6)	SS: BC-SC-MC-TC-SCRSH	P_{CL}
9	SW + normal pressure 343 PSI (bolts + rock-concrete adhesion)	BC: TC-BC-SC-BCRSH-TCRSH-MC-CL	$P_{MC}+0.2(P_{CL}- P_{MC})$
10	SW + normal pressure 23 PSI (with and without openings)	BC: CC-MC-TORCH-BCRSH-BOCRSH-CL (openings)	P_{CL}
11	SW + normal pressure 5 PSI (φ=0.7)	BC: MC-TCF-BCF-SF-BF-TF	/
12	SW + normal pressure 5 PSI (φ=0.7)	BC: MC-(TC+BC)-MCRSH-BCRSH-UMCR-SCRSH-CL	P_{CL}
13	SW + normal pressure 35 & 39 PSI	SS: MC-(TC+BC)-MCRSH-BCRSH-UMCR-SCRSH-CL	/
14	SW + normal pressure 20 PSI (FS=1.6)	BC: MC-CL	P_{CL}
15	SW + normal pressure 50 PSI (FS=1.1)	SS: YP-CL	P_{CL}
16	SW + normal pressure 50 PSI (FS=1.1)	SS: YP-CL	P_{CL}
17	SW + normal pressure 20 PSI (FS=1.0)	SS: YP-CL	P_{CL}
18	SW + normal pressure 70 kPa (FS=1.0)	SS: YP-CL	P_{CL}
19	SW + normal pressure 140 kPa (FS=1.5, 2.0)	No damage	/
20	SW + normal pressure 14 & 35 kPa (with bolts)	BC: MC-CL	P_{CL}
21	SW + normal pressure 2 & 5 PSI (φ=0.7)	BC: MC-MCRSH-UMCR-BCRSH-TCRSH-CL	P_{CL}

Legend: SW - self-weight, HP - hydrostatic pressure
BC – bending cracking failure, TC- first top cracks, BC – first bottom cracks, SC – first side cracks,
MC – first middle cracks, CL – collapse (or end of analysis), SS – shear-slip failure on the contact, BCRSH – first bottom crush, TCRSH – first top crush, CC – corner cracks, TOCRSH – top opening crush, BOCRSH – bottom opening crush, TCF – first top corner fracture (ε_u reached),
BCC – first bottom corner fracture (ε_u reached), SF – first side fracture (ε_u reached),
BF – first bottom fracture (ε_u reached), TF – top fracture (ε_u reached), MCRSH – middle crush,
UMCR – ultimate middle cracks ((ε_u reached)), SCRSH – side crush, YP – yield point,
P_{CL} – collapse pressure, P_{TC} – first top cracks pressure, P_{MC} – first middle cracks pressure

The consistency of the obtained results using the backward-Euler return method can be clearly seen by the obtained diagrams of principal stresses and principal strains. For example, in Fig. 7, a representative $\sigma_1 - \varepsilon_1$ diagrams in principal directions (tension) is shown, selected from the results of the analysis of a

Proceedings of the 2nd Croatian Conference on Earthquake Engineering - 2CroCEE
Zagreb, Croatia - March 22 to 24, 2023
Copyright © 2023 CroCEE
DOI: https://doi.org/10.5592/CO/2CroCEE.2023.26

plate with bolts (study case no. 6) from where the mathematical consistency of the principal stress σ_1 update is evident.

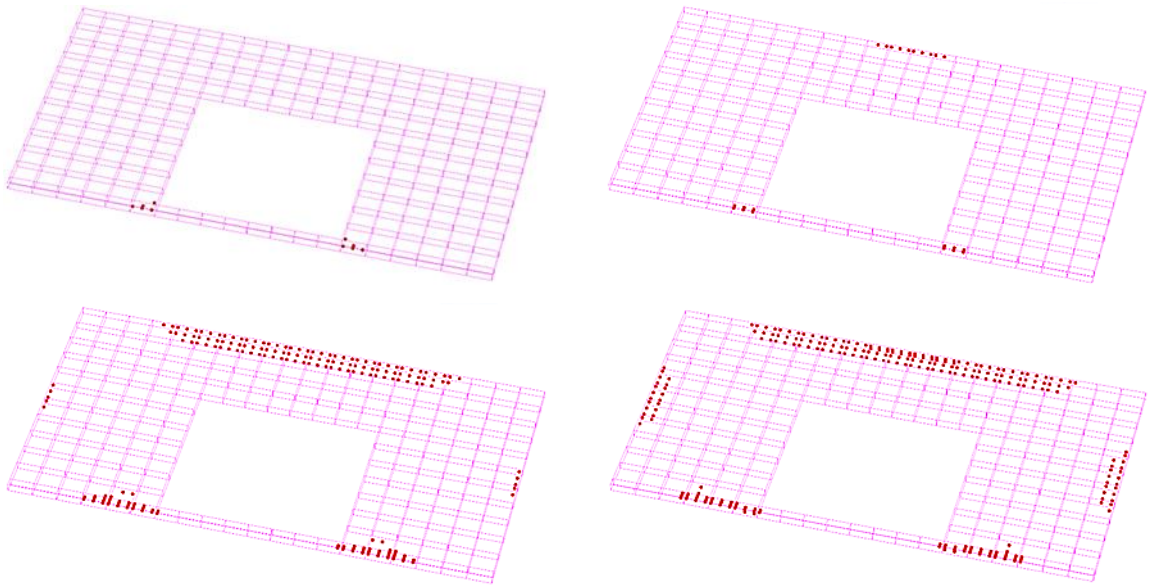

Figure 3. Study case 4, mine seal with opening: Critical steps of PFM (red dots denote cracks)

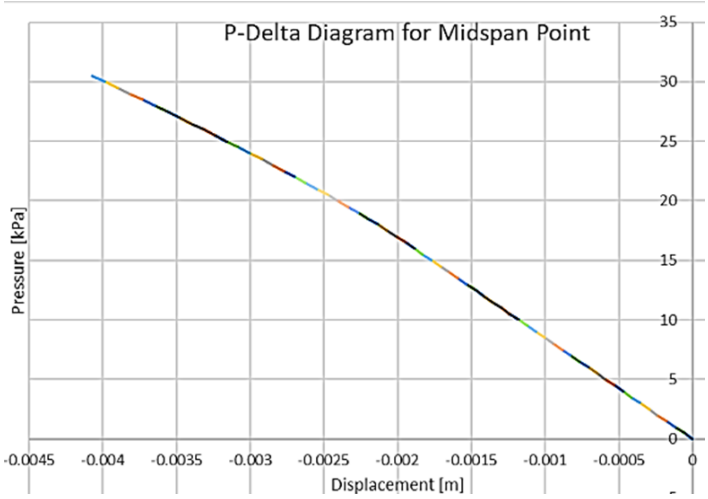

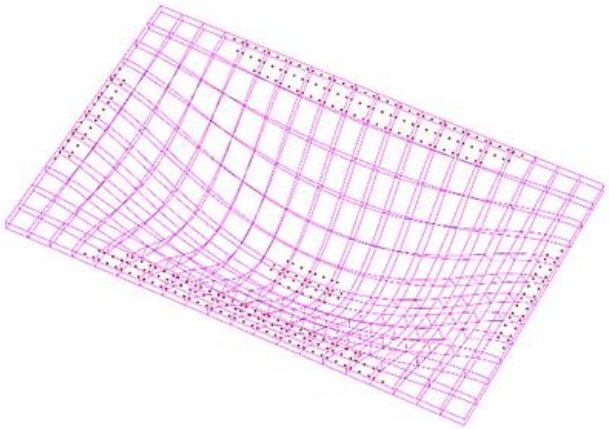

Figure 4. Study case no. 5, mine seal without openings: Obtained force-displacement curve and final step of PFM (red dots denote cracks)

Proceedings of the 2nd Croatian Conference on Earthquake Engineering - 2CroCEE
Zagreb, Croatia - March 22 to 24, 2023
Copyright © 2023 CroCEE
DOI: https://doi.org/10.5592/CO/2CroCEE.2023.26

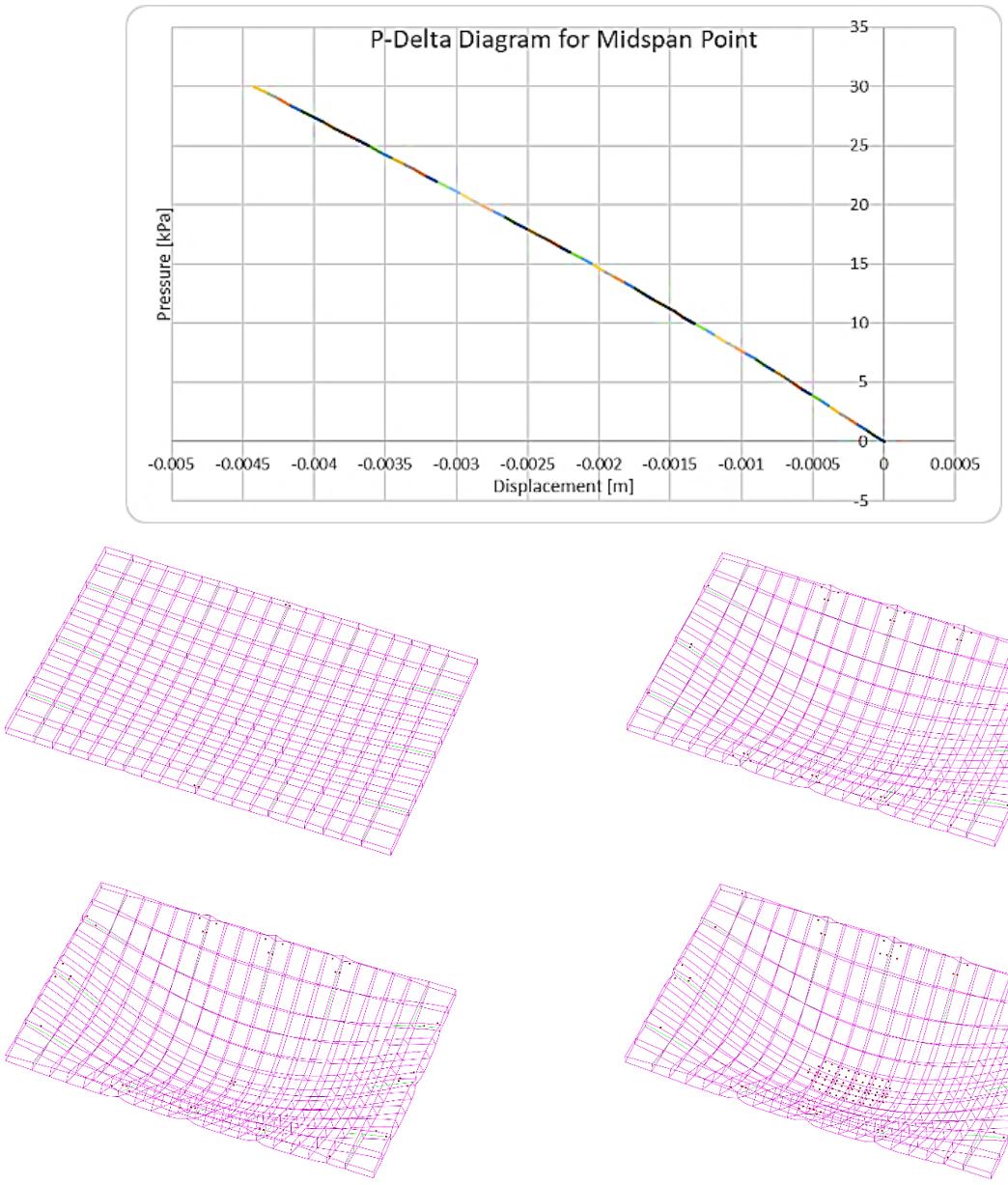

Figure 5. Study case no. 5 mine seal with bolts: Obtained force-displacement curve and critical steps of PFM (green lines denote bolts, while red dots denote cracks)

5. Conclusions

Mine seals are structures used to serve as protection shields against short term instantaneous pressure loadings like blasts, which could occur in mine cells during the excavation period. With the recent technical norms, the level of seal design safety requirements has been increased. In addition to other safety measures, these requirements can be satisfied if the seal design includes FEM nonlinear analysis. In the paper, the authors' experience in modelling and analysis of mine seal structures is briefly presented. From that point of view, the following conclusions can be made:

(1) According to results obtained from tests (that are not the subject of this paper), the new technological materials like Flexus, Rocksil, Silcrete etc, have been proved to have properties that can be well simulated by the Willam-Warnke and Drucker-Prager plastic criteria. Hence, the selected elastic-plastic material models implemented in the FELISA/3M software can realistically simulate the progressive failure mechanism of mine seal structures in practice.

Proceedings of the 2nd Croatian Conference on Earthquake Engineering - 2CroCEE
Zagreb, Croatia - March 22 to 24, 2023
Copyright © 2023 CroCEE
DOI: https://doi.org/10.5592/CO/2CroCEE.2023.26

(2) The implemented backward-Euler return method with the consistent tangent modular matrix has shown computational stability and fast convergence compared to the forward-Euler return method used in many contemporary software packages.

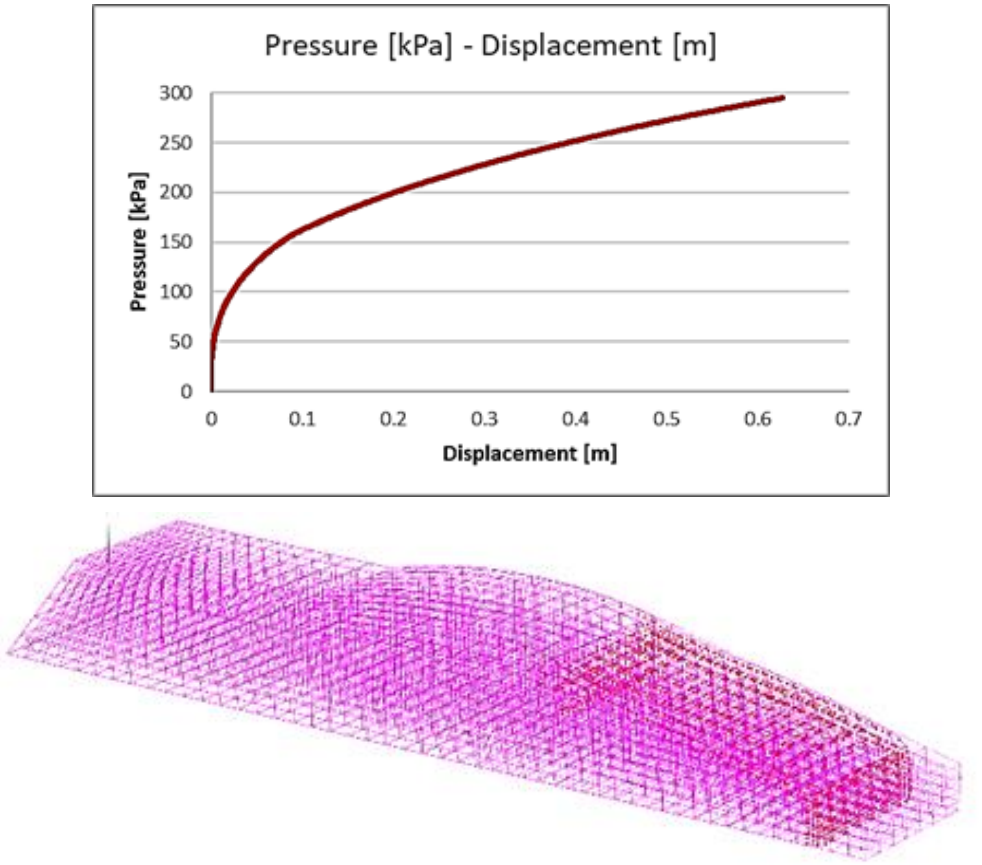

Figure 6. Study case no. 16: FEM Obtained force-displacement curve and final step of failure mechanism (red dots denote points where principal shear stresses exceed allowable values)

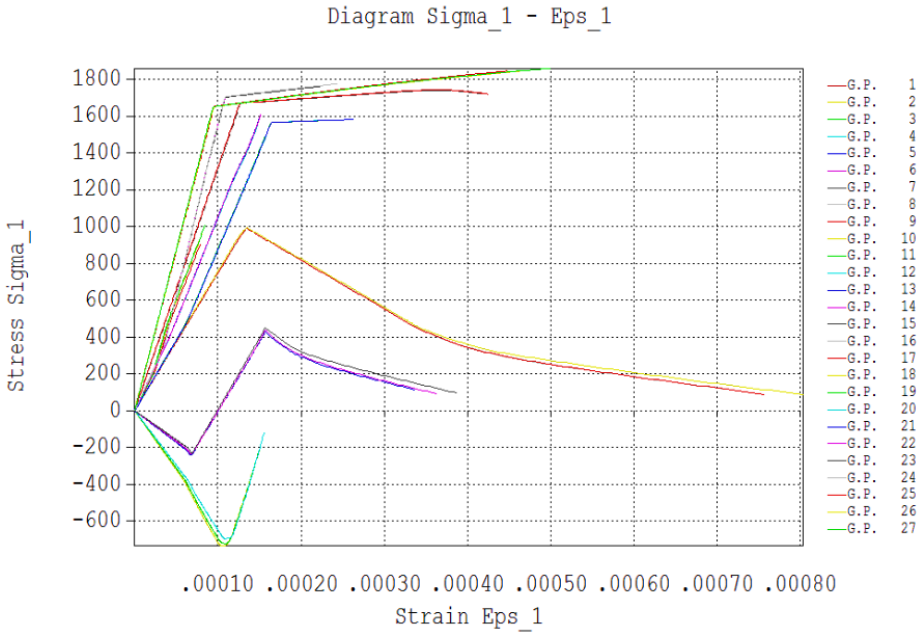

Figure 7. Obtained principal $\sigma_1 - \varepsilon_1$ diagrams for all 27 Gaussian points of a characteristic element, study case no. 6, plate structure with bolts

Proceedings of the 2nd Croatian Conference on Earthquake Engineering - 2CroCEE
Zagreb, Croatia - March 22 to 24, 2023
Copyright © 2023 CroCEE
DOI: https://doi.org/10.5592/CO/2CroCEE.2023.26

(3) Basically, two types of mine seal structures have been modelled: (1) Rectangular plates (with/without openings and with/without bolts), and (2) Dam-like mine seal structures built of Silcrete foam. The first type of structures usually failed in bending mode, while those of the second type usually failed in shear-slip mode. Structures of the first type were modelled by the Willam-Warnke yield criterion, while those of the second type were modelled by the Drucker-Prager yield criterion. The collapse of the structure (i.e., the end-of-analysis due to divergence indicating failure) was usually adopted as a design criterion for the plate mine seal structures. However, sometimes, different expressions were adopted, depending on the developed damage. On the other hand, the onset of the large shear-slip deformation (or the ultimate points when the analyses usually diverged and stopped) was adopted as a design criterion for dam-like mine seal structures.

(4) Two main tasks were performed in the analyses. The first task referred to the case of known material strength, so that the thickness of the seal had to be defined for the given loading level. The second task referred to an unknown material strength so that it had to be defined for the known loading level and thickness.

(5) Because the materials for mine seal structures are still developing, further investigation on their modelling is needed.

References

[1] Zipf, R.K. Jr., Mohamed, K.M., McMahon, G.W. (2009): Design and Analysis of a New Method to Test Mine Seals. *Proceedings of the 80th Shock and Vibration Symposium (DoD)*, San Diego, California, October 25-29, 2009. Virginia: The Shock & Vibration Information Analysis Center,1-17.

[2] Kallu, R.R. (2009): *Design of reinforced concrete seals for underground coal mines*. Ph.D. Dissertation, College of Engineering and Mineral Resources, West Virginia University, Morgantown, West Virginia.

[3] Willam, K.J. and Warnke, E.P. (1974): Constitutive Model for the Triaxial Behaviour of Concrete. *Proceedings, IABSE Seminar on "Concrete structures subjected to triaxial stresses" 17-19 May 1974*, ISMES, Bergamo, Italy. http://dx.doi.org/10.5169/seals-17526 .

[4] ASCE (1982): *State-of-the-Art Report on Finite Element Analysis of Reinforced Concrete*. New York.

[5] Chen, W.F. (1982): *Plasticity in Reinforced Concrete*. McGraw-Hill Book Company.

[6] Chen, W.F., and Saleeb A.F. (1994): *Constitutive Equations for Engineering Materials", Volume 1: Elasticity and Modelling*. Elsevier. [7] Chen, W.F., and Saleeb A.F. (1994): *Constitutive Equations for Engineering Materials", Volume 2: Plasticity and Modelling*. Elsevier.

[8] Owen, D.R.J., Hinton, E. (1980): *Finite Elements in Plasticity, Theory and Practice*. Pineridge Press Limited, Swansea, UK.

[9] Crisfield, M.A. (1991): *Non-linear Finite Element Analysis of Solids and Structures, Volume 1: Essentials.* John Wiley & Sons.

[10] Crisfield, M.A. (1997): *Non-linear Finite Element Analysis of Solids and Structures, Volume 2: Advanced Topics*. John Wiley & Sons.

[11] FELISA/3M (2022), *General purpose software package for analysis of structures*, UKIM-IZIIS, 1990-2022